A Hypersonic Flow Model for the Aid of Conceptual Design of Re-Entry Vehicles

Scott Bagwell and Ken Morgan
Civil and Computational Engineering Research Centre
College of Engineering
Swansea University
Swansea UK
638988@swansea.ac.uk

Abstract—The aim of this project is to produce a low fidelity mathematical model that can rapidly simulate geometries under hypersonic flow regimes using Newtonian flow theory. A panelling method has been employed to evaluate the effects of hypersonic flow regimes on the aerodynamic performance of a number of 2D geometries. The model was first validated for a cylinder, where the analytical solution is known. The results obtained from this study were then compared with the analytical solution to understand the behaviour of the convergence rate under h refinement of the mesh. The model was found to provide a first order approximation. A selective discretisation re-panelling algorithm was developed to reduce the computational expense of the program. The convergence rate of this algorithm was also studied for the cylinder problem. The results suggested that, while the h-refinement of the mesh under this scheme produced the same convergence rate as the linear panelling method, the convergence rate with respect to the number of elements in the mesh was improved. These findings suggest that the use of such selective discretisation algorithms are beneficial in creating smaller meshes while still capturing the same level of accuracy and reducing the computational requirements. In addition, this project looks at the implementation of this model for 3D applications. In this case, the starting point is a suitable discretisation of the body's surface using a surface meshing technique. The convergence rate was again studied for hypersonic flow over a sphere. The problem of the model was shown to be first order accurate for the 3D case. The capability of the model was demonstrated for a full 3D aircraft configuration.

1 Introduction

Hypersonic flight has been an active area of research since the late 1940s with the introduction of rocket flight. The number of space flight missions is expected to rise over the next few decades with the increase in space exploration and the introduction of commercial spaceflight. Most of these flights will involve traversing the altitude of 100km above mean sea level, known as the Kármán line [1]. This is the internationally accepted boundary of the atmosphere and the point at which spaceflight begins.

Computational simulation of hypersonic aerodynamics plays an important role in the efficient design and development of space craft. A particular area of interest in designing these vehicles is their re-entry into the atmosphere at speeds in excess of Mach 5, the generally accepted threshold for hypersonic flight [2], shown in Figure 1. During the design phase of atmospheric re-entry vehicles, an iterative process is employed to analyse the performance of a number of aerodynamic shapes under the expected hypersonic flow conditions [3] [4]. However, the computational requirements of high fidelity models for hypersonic flow are usually significant. For this reason the use of lower fidelity models is generally accepted, to reduce computational requirements. Panel methods are often employed during this phase due to their ability to readily represent arbitrary shapes.

Fig. 1: Command Module re-entering the atmosphere [5]

The aim of this project is to design a hypersonic aerodynamic computer model capable of simulating arbitrary geometries under hypersonic flow regimes, based upon the Newtonian flow model. This will be developed through the use of MATLAB in order to construct a computer program that can rapidly simulate these flow conditions for a defined shape, which will provide a useful tool in the concept design phase of re-entry vehicles. The project will also study the numerical capabilities of the program, by validating the model against known analytical solutions, in order to determine the accuracy of the results and the extent of its applicability.

2 METHOD

2.1 Newtonian Flow Model

To analyse hypersonic flow around arbitrary geometries, a mathematical model has to be defined that is capable of capturing the phenomena inherent in such flow regimes. The mathematical model chosen to analyse the flow parameters in this project is the Newtonian flow model [6]. This model analyses the basic dynamics of a fluid without considering the complexities of the Navier-Stokes equations [2], the fundamental governing equations of all fluid dynamics problems. Newton's theory states that when fluid impacts a surface the momentum in the normal direction acts as a force on the surface, while the momentum in the tangential direction is conserved. The transfer of momentum produces a pressure on the surface, from which the aerodynamic coefficients can be obtained.

Newton's model assumes that the flow is a directed rectilinear movement of particles in stream lines, unlike current models which describe flow behaviour as a random and structured motion of particles known as molecular motion. This assumption of rectilinear motion gives rise to an effect known as the shadowing effect [7]. This effect means that surfaces not facing the flow direction are shadowed and do not experience any change in momentum as the flow cannot curl round surfaces and impact them from behind. This results in a zero pressure change from the free stream in these shadowed regions, or $p = p_\infty$, which results in a zero pressure coefficient, which can be seen in Figure 2.

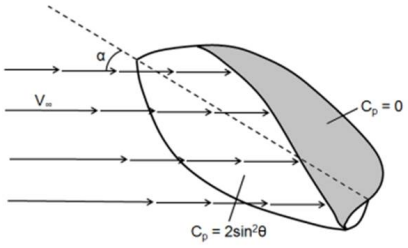

Fig. 2: Shadowing of flow particles [7]

To illustrate the mechanics of this method, consider a flat plate, inclined at an angle θ to the horizontal. Apply a control volume to the fluid for the projected region (sine component) of the plate surface, as shown in Figure 3.

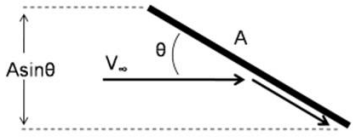

Fig. 3: Control volume of flat plate [7]

The normal velocity component can be expressed as

$$V_n = V_\infty \sin\theta \tag{1}$$

and the volumetric flow rate within the control volume can be calculated as

$$Q = VA = V_\infty A \sin\theta \tag{2}$$

Applying Newtons second law of motion which concedes that the rate of change of momentum normal to the plate produces a force on the plate surface. This force can then be derived as

$$F_n = \frac{\mathrm{d}(mv)}{\mathrm{d}t} = \rho Q V_n = \rho_\infty V_\infty^2 A \sin^2\theta \tag{3}$$

From this, the pressure on the surface can be calculated as

$$p = \frac{F_n}{A} + p_\infty = \rho_\infty V_\infty^2 \sin^2\theta + p_\infty \tag{4}$$

The pressure coefficient for the flat plate can be calculated by taking the pressure differential between the surface and the free stream and normalising the value with respect to the far field dynamic pressure q_∞.

$$C_p = \frac{p - p_\infty}{q_\infty} = \frac{\rho_\infty V_\infty^2 \sin^2\theta}{1/2\,\rho_\infty V_\infty^2} = 2\sin^2\theta \tag{5}$$

From the pressure coefficient, the expressions

$$C_d = \frac{D'}{qA} = \frac{F_n \sin\theta}{qA} = C_p \sin\theta = 2\sin^3\theta \tag{6}$$

$$C_l = \frac{L'}{qA} = \frac{F_n \cos\theta}{qA} = C_p \cos\theta = 2\sin^2\theta\cos\theta \tag{7}$$

The Drag and Lift coefficients can also be calculated by taking the 2D drag D' and lift L' forces as components of the normal force.

2.2 Modified Newtonian Model

The model can be extended to incorporate some of the physical phenomena inherent in hypersonic flight, such as shock waves. This can be done by carrying out analysis of the flow parameters across the shock, by assuming a suitable control volume. Consider hypersonic flow over an arbitrary body, as shown in Figure 4.

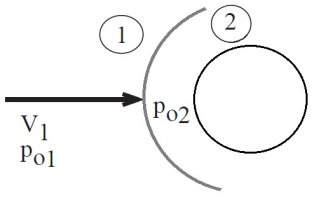

Fig. 4: Bow shock around a cylinder

The pressure at any point on the surface in the Newtonian model, is given by

$$p - p_\infty = \rho_\infty V_\infty^2 \sin^2\theta \tag{8}$$

The pressure at the stagnation point behind the shock wave p_{02}, where the local surface inclination is $90\,^\circ$ and as a result $\sin\theta = 1$, is therefore given as

$$p_{02} - p_\infty = \rho_\infty V_\infty^2 \tag{9}$$

This means that the coefficient of pressure at the stagnation point, $C_{p,max}$ is given by

$$C_{p,max} = \frac{p_{02} - p_\infty}{1/2\rho_\infty V_\infty^2} \tag{10}$$

The coefficient of pressure on the surface downstream of the stagnation point follows the Newtonian sine-squared variation, given by equation (5). Therefore the pressure coefficient across the surface under hypersonic flow can be obtained as

$$C_p = C_{p,max} \sin^2\theta \tag{11}$$

In the hypersonic flow around the body a shock wave develops on the leading edge. The shock at this point, given that the shape has a suitably large Mach cone, can be treated as a normal shock and so the stagnation pressure p_{02} on the surface, behind the shock, can be determined. From the ideal gas law $\rho = p/R_g T$, the Mach relation $M = V/c$ and the speed of sound relation $c = \sqrt{\gamma R_g T}$, where γ is the specific heat ratio, the coefficient of the stagnation pressure can be redefined as

$$C_{p,max} = \frac{2}{\gamma M_\infty^2}\left(\frac{p_{02}}{p_\infty} - 1\right) \tag{12}$$

From the normal shock relations, the ratio of the stagnation pressure on the surface of the body to the freestream pressure is given by the Rankine-Hugoniot relation

$$\frac{p_{02}}{p_\infty} = \left(\frac{(\gamma+1)^2 M_\infty^2}{4\gamma M_\infty^2 - 2(\gamma-1)}\right)^{\frac{\gamma}{\gamma-1}} \left(\frac{(1-\gamma) + 2\gamma M_\infty^2}{\gamma+1}\right) \tag{13}$$

This equation can be used to determine the pressure ratio for given flight speeds, or Mach numbers. This can be used in the modified Newtonian relation, equation (12), to calculate the pressure coefficient on the surface.

Now consider the flow across an oblique shock wave. The exact oblique shock relation for the coefficient of pressure is given as

$$C_p = \frac{4}{\gamma+1}\left(\sin^2\beta - \frac{1}{M_\infty^2}\right) \tag{14}$$

As the freestream Mach number tends towards infinity, $M_\infty \to \infty$, and the specific heat ratio tends toward 1, $\gamma \to 1$, equation (14) reduces to

$$C_p = 2\sin^2\beta \tag{15}$$

This result is obtained from shock wave theory and so does not link to the description of Newtonian theory. However, now consider the effect of the Mach number on the shock wave; as $M_\infty \to \infty$ the shock wave approaches the surface of the body and thus $\beta \to \theta$. Applying this to equation 15 results in the Newtonian sine-squared law, equation 5. This suggests that as $M_\infty \to \infty$ and $\gamma \to 1$ the problem can be exactly described by the Newtonian sine-squared law.

2.3 Panel method

To solve a full problem a numerical discretisation method must be applied to represent complex geometries. A panel method is used to discretise the geometry surface, in which the surface is modelled as a series of flat plates (panels), to which the Newtonian flow theory can be applied. An example of the application of panelling method for a double ellipse [3] [8] is shown in Figure 5.

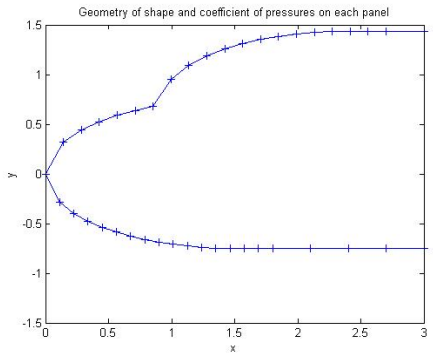

Fig. 5: Crude panelling of the double ellipse

2.4 Computer Model

In order to produce accurate results for the numerical solution to a problem, a great number of elements (or panels) are required to accurately capture the geometry and produce significantly converged results. MATLAB was used to create a computer program capable of carrying out the vast number of calculations on these dense meshes needed for complex geometries. This program is based on an h-refinement scheme where the number of panels is increased, and simultaneously the size of each panel (h) is decreased, with each iteration to increase the accuracy of the surface representation. The error in the solution is measured as the difference between the solution of the current, finer mesh with the solution of the previous mesh. This process of reducing

the size of the panels is repeated, where the error in the solution reduces, until the desired accuracy is reached. This approach demonstrates the numerical convergence of the procedure and the convergence parameter chosen is the drag coefficient, as it is non-zero in nature for all bodies including symmetric (such as the circle and sphere).

A number of geometries have been included in the code as pre-defined configurations. They use derived analytical relationships in order to accurately define the shapes for discretisation. These geometries include:

1) cylinder
2) ellipse (inc. user input height ratio)
3) NACA 4 series aerofoils
4) double ellipse (shown in fig. 5)
5) Schematic apollo command module [4]

Users may also input geometries using data points created from drawings etc. This method uses a third order spline function to more accurately capture inputs with limited data points. This is achieved through the inclusion of user generated .txt files or other input file methods. An input Excel file has been provided as part of the code to which users can create their own geometries, an example of which is included with the code for the cylinder.

2.5 Selective Refinement Algorithm

A problem incurred with the application of a panel method to this model is the effect of shadowing. Certain geometries have large sections that are shadowed and do not experience a direct impact with the flow, resulting in zero surface pressure. Accurately capturing the geometry in these regions is therefore not required and so no re-panelling is needed beyond the initial discretisation.

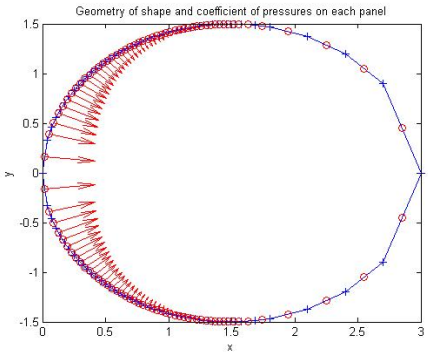

Fig. 6: Selectively re-panelled cylinder

A method of selectively re-panelling a surface, based on the pressure coefficient, is required to reduce the level of computational requirements on each mesh. Figure 6 shows this selective procedure applied to a circular cylinder. This clearly demonstrates the absence of re-panelling in the shadowed region, on the right hand side of the circle for x between 1.5 and 3. The red arrows show the magnitude of the pressure coefficient on each panel as vectors plotted at their centre points.

Initially a coarse mesh is used to represent the geometry surface. In the program, this is normally achieved using 20 panels as an initial discretisation. The Newtonian method is applied to this initial geometry in order to determine the pressure coefficients on each panel. These results are used to determine the panels which lie in the shadowed region and those that indicate surface pressure. The panels where the pressure is non-zero are then linearly re-discretised into a set of smaller panels. The zero pressure panels directly adjacent to these non-zero regions are also captured into this re-discretisation programme to identify any loss in accuracy of the surfaces due to initial course meshing. The process is repeated until the desired convergence level is reached.

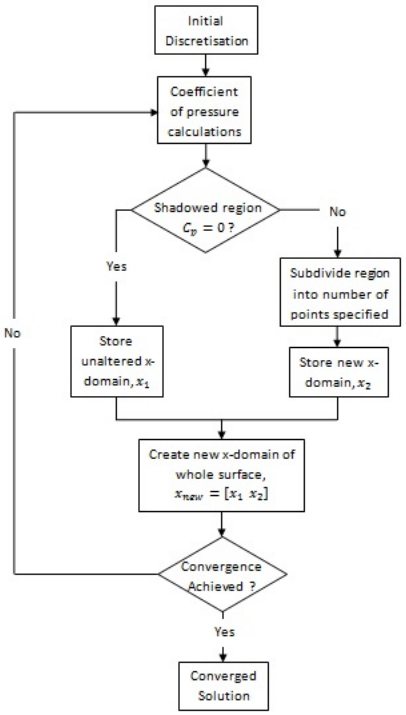

Fig. 7: A Flowchart of the selective re-panelling algorithm

This flowchart, Figure 7, describes the logic steps of the re-panelling algorithm and how each stage is built into the overall procedure.

2.6 3D Application

During this project, the extension of the Newtonian flow model to 3D applications has been investigated.

To apply a suitable panelling method to these 3D applications a surface meshing technique has been developed. This technique starts by generating a set of points on the surface, through the analytical solutions, of certain pre defined 3D shapes. These geometries include:

1) sphere
2) ellipsoid (inc. height/width/depth ratio)
3) NACA 4 series finite wings (with taper ratio)

The points are then meshed using the Delaunay triangulation method to create the 3D panels (elements) as triangles on the surface of the shape. This method uses the mathematical relation of circumcircles of the points to create the triangular elements. The vertices of each element coincide with the points, which are suitably spaced to maximise the minimum angle and avoid skinny elements. This information is stored in an array known as the connectivity table. The elements and the triangulation (or connectivity) data are used to define the surface mesh of the shape. The surface is analysed using vector algebra and the surface normals computed. This allows the calculation of the pressure coefficients and shadowed regions on the surface. Figure 8 shows the triangulated surface mesh of a sphere and the surface normals plotted at the centroids of each element, as well as the defined freestream vector (red arrow).

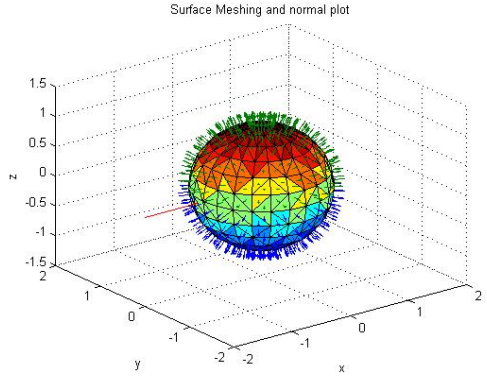

Fig. 8: Surface mesh of sphere with surface normals

3 Results

3.1 Numerical Convergence

To verify that the model is accurate, a geometry with a known analytical solution is simulated initially. For the 2D case, a number of geometries, such as the flat plate, have an analytical solution but perhaps the most widely used is that of the circle. The analytical solution for the lift and drag coefficients of the circle can be obtained by integrating the pressure coefficient across the surface, which yields $C_d = 4/3$ and $C_l = 0$.

The measure of numerical convergence of the solutions has been studied to validate the accuracy of the model. It is also used to confirm the applicability of the selective refinement algorithm to this model by comparing the initially employed linear refinement scheme with the developed selective scheme. The computer model is based around an h-refinement scheme which decreases the size of each panel h, thus increasing the number of panels N in the mesh in order to achieve smaller errors that converge towards the exact solution. Consider the following definitions

$$E \approx h^n \qquad and \qquad E \approx \frac{1}{N}^n \tag{16}$$

where E is the error of the model, h is the smallest element size, N is the number of elements and n is the order of convergence of the scheme. Studying first the relationship of h, by taking the natural logarithm of equation 16 and rearranging for n it follows that

$$n \approx \frac{\log E}{\log h} \tag{17}$$

By obtaining the data for element size and error at each iteration the numerical convergence can be plotted. Figure 9 shows the logarithmic plot of the variation of the error in the solution, with respect to the analytical solution, for a circle.

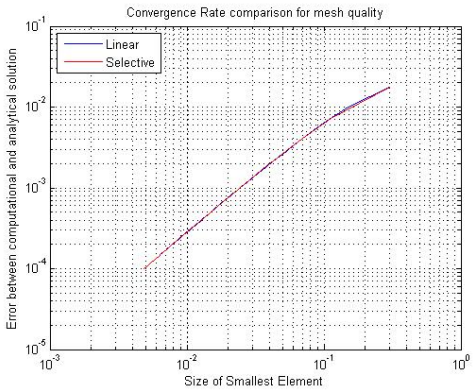

Fig. 9: Numerical convergence for mesh size (h)

By determining the gradient of this relationship the order, n, of the model can be determined. This plot compares the convergence of both the selective and linear refinement schemes. The order is calculated to be 1.3146 for both schemes. This suggests that the error inherent in the model is approximately of order h, $E \approx O(h)$.

A similar study can be carried out with the comparison of number of elements in the mesh N. By studying equation (16), this time, with respect to N the order of the model can be obtained as

$$n = -\frac{\log E}{\log N} \tag{18}$$

By again measuring the error the convergence could be plotted, shown in Figure 10.

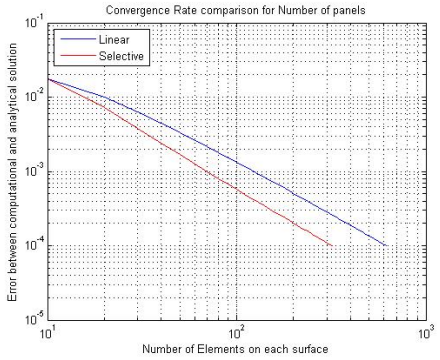

Fig. 10: Numerical convergence for no. of elements (N)

This plot shows that the order of convergence, with respect to N for the linear refinement scheme, differs from that of the selective scheme. The linear scheme produces an order of 1.3146 and suggest the error $E \approx O(1/N)$, because of the negative gradient of the curve. However the selective refinement scheme produces an order of 1.4948. This is shown in the plot where the linear scheme used 2950 elements to converge to an error of $< 10^{-5}$, whereas the selective scheme used only 1490 to converge to the same accuracy.

For 3D applications the analytical solution for the sphere can be obtained by integrating the pressure over the surface. This yields $C_D = 1$ and $C_L = 0$. The numerical convergence study can be carried out in much the same way as the 2D case. The solution to the sphere converged to an error of $< 10^{-6}$ with 4488 elements in the mesh. Figure 11 and Figure 12, show the convergence of the h-refinement and number of elements N respectively.

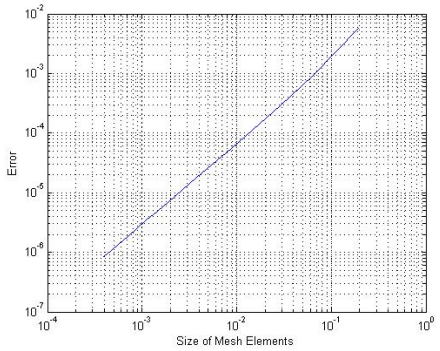

Fig. 11: 3D numerical convergence for h

The order of the h refinement scheme in the 3D application is calculated to be 1.4207.

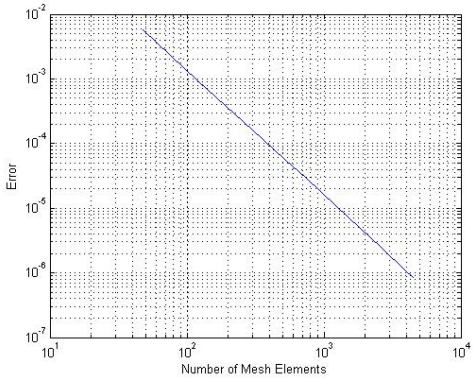

Fig. 12: 3D numerical convergence for N

The order of the N scheme is calculated to be 1.9410. This could be improved further by applying the selective refinement algorithm to the 3D case.

3.2 Pressure Distribution

From the Newtonian model, the pressure coefficient on the surface of the geometry can be calculated. By plotting the pressure on each panel as a vector, with the panel mid point as the origin, the graphical representation of the pressure magnitude on the geometry surface can be obtained. This is shown on the quiver plot in Figure 13.

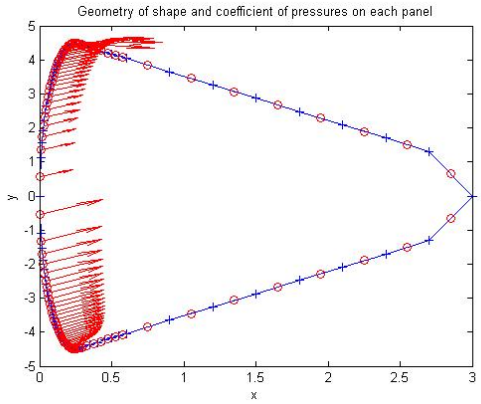

Fig. 13: Pressure vector plot for the Apollo command module configuration at 45° angle of attack

By plotting the values of the surface pressure against the mid points of the panels, a variation of pressure along the surface of the geometry can be visualised. Figure 14, shows the pressure distribution for a NACA4412 airfoil at 20° angle of attack where the two lines indicate the pressure on the upper and lower surfaces.

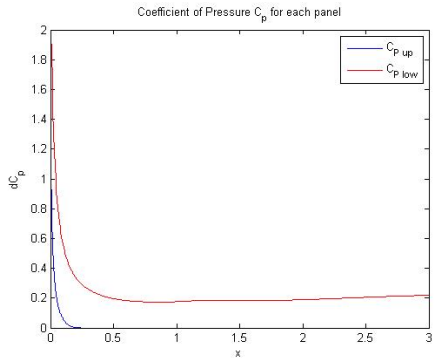

Fig. 14: Surface pressure plot of the NACA4412 at 20° angle of attack

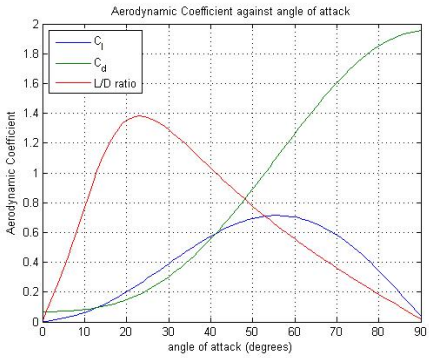

Fig. 16: Aerodynamic coefficients against angle of attack for NACA0012

This idea was carried forward to the 3D model. Due to the nature of 3D geometries, a more complex method for plotting the surface pressure distribution is required to capture the aerodynamic behaviour of the entire surface for hypersonic flow. Surface plots were used to determine the pressure distributions across the shapes by applying a colour to the surface of each element according to the value of pressure. An example of these plots can be seen in Figure 15 with the colour bar, which shows the value assigned to each colour, displayed to the right of the plot.

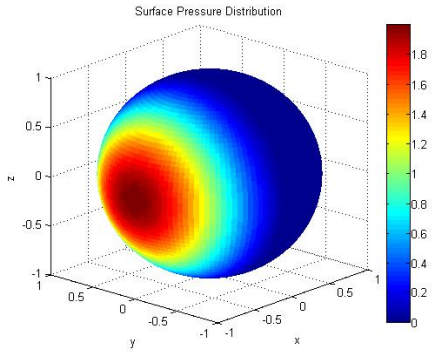

Fig. 15: Surface Pressure plot for a sphere

3.3 Aerodynamic Behaviour

From the distribution of the pressure across the surface of the geometry; the aerodynamic characteristics, lift and drag coefficients can be determined. Using these coefficients the lift-to-drag ratio can also be plotted to determine the performance angle of the geometry. These were then plotted against an angle of attack range to determine how the aerodynamics of these 2D cross sections vary with angle of attack. Figure 16 shows the lift and drag coefficients and the lift-to-drag ratio as a function of angle of attack for a NACA0012 airfoil.

This capability of allowing the angle of attack to be varied was also included in the 3D application. However with 3D geometries, not only does the angle of attack change the aerodynamic performance of the geometry but also a sideslip (or yaw) angle may be present. This has been incorporated into the model but, due to the interrelation of the two angles, a simple line plot is computationally expensive to produce. The model allows for user input of these angles in order to produce the surface plots, but does not produce a sweep through a range of angles.

3.4 Modified Newtonian Results

With data obtained from the modified Newtonian model, discussed in section 2.2, the effects of the flow speed and conditions can be included into the analysis. This definition of pressure coefficient at the stagnation point $C_{p,max}$, given by the equations (12) and (13), depends upon the Mach number and specific heat ratio. By varying these quantities different flow regimes around the aerodynamic body can be studied.

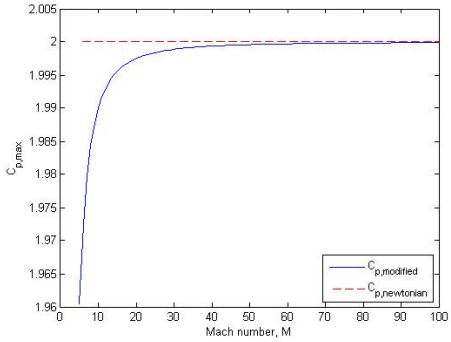

Fig. 17: $C_{p,max}$ variation with M

Figure 17 illustrates the variation of the maximum pressure coefficient with the Mach number M. The plot varies

between a Mach number of 5, to comply with the general definition of a hypersonic flow regime (stated in section 14 of Anderson's book [2]), and 100, to limit the number of data points studied. The plot shows that $C_{p,max}$ tends towards 2 (red dashed line on the graph), decaying exponentially as M tends towards infinity, resulting in the simple Newtonian theory shown in section 2.1.

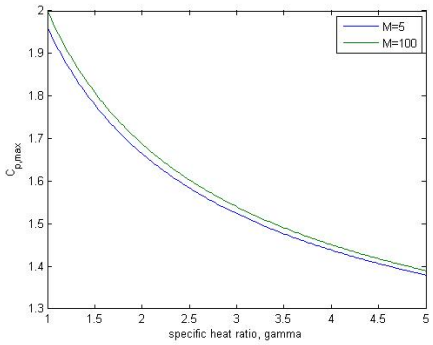

Fig. 18: $C_{p,max}$ variation with γ

Figure 18 shows the variation of the maximum pressure coefficient with the specific heat ratio γ. The plot varies between a γ of 1 and 5, again to limit the total number of data points. The plot shows that $C_{p,max}$ tends exponentially towards 2 as γ tends towards 1 for a Mach number towards infinity, resulting in the simple Newtonian model. Also illustrated on the plot is the variation of $C_{p,max}$ for a Mach number of 5, the limit of hypersonic flight, on the lower line. This range in the variation of $C_{p,max}$ with Mach number, for a given γ, also reduces as the specific heat ratio tends towards infinity, shown by the squeezing of the two lines.

This study suggests that the Newtonian flow model is the theoretical upper limit of the full modified Newtonian model, which complies with the theoretical analysis discussed at the end of section 2.2.

3.5 Complex Configurations

The model was tested using a 3D surface geometry of the Dassault Falcon aircraft. This was done to demonstrate how the model copes with complex geometries that require large meshes consisting of a number of elements in the order of 10^6. The data files of the meshes, obtained, offered a full volumetric domain mesh with both the aircraft and free stream surface boundaries defined. Some pre-processing was carried out to recover only the surface mesh of the aircraft, ignoring the outer boundary, and saving these meshes into new data files for computation. The coarsest mesh produced is illustrated in Figure 19, where the aircraft layout is clearly visible. This mesh consists of 42720 elements. Other meshes containing 534092 and 1201860 elements are also studied.

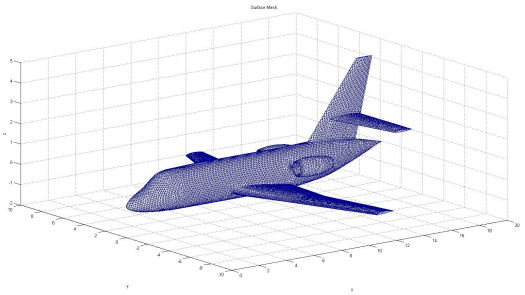

Fig. 19: Surface mesh of Falcon

A comparison between the available mesh qualities is given by Figure 20. This figure shows a zoomed section of the aircraft on the engine nacelle and shrouding, which requires a high level of detail due to its complex geometry. Figures 20a and 20b show the surface representation of the coarsest and finest mesh respectively.

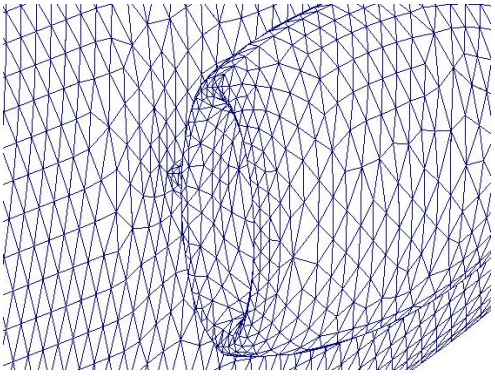

(a) Mesh of 42720 elements

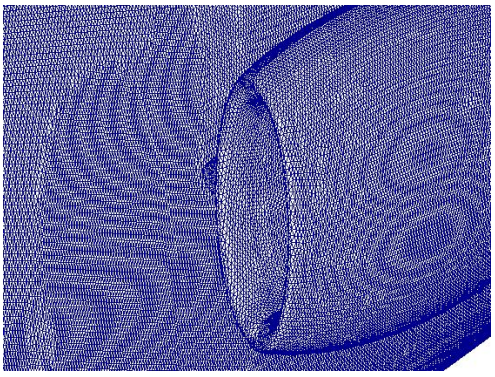

(b) Mesh of 1201860 elements

Fig. 20: Detail of surface meshes

From the surface mesh the pressure coefficient on each panel can be calculated using the local surface inclination of each surface element. The resulting surface pressure

plot, for a 60 ° angle of attack and 30 ° sideslip (yaw) angle with a mesh of 42720 elements, is shown in Figure 21.

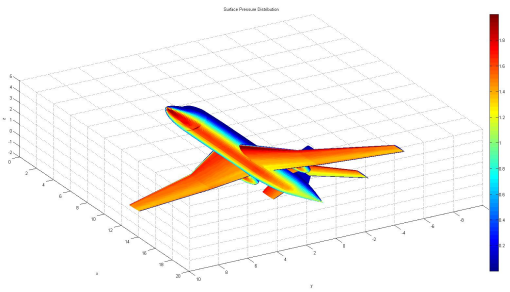

Fig. 21: Pressure distribution of Falcon

A comparison between the meshes was also carried out with the pressure distribution plots to show the effects of the coarseness of the mesh on the resolution of the surface distribution. This is shown in Figure 22, where Figure 22a and 22b show the representation of the coarsest and finest meshes respectively.

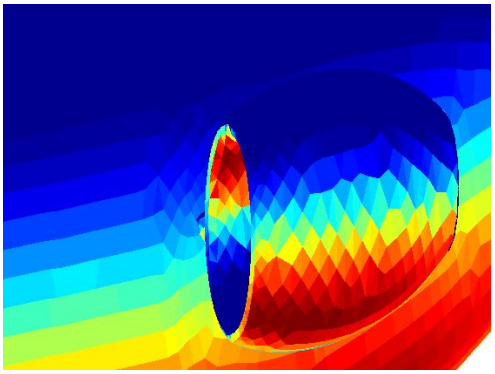

(a) Mesh of 42720 elements

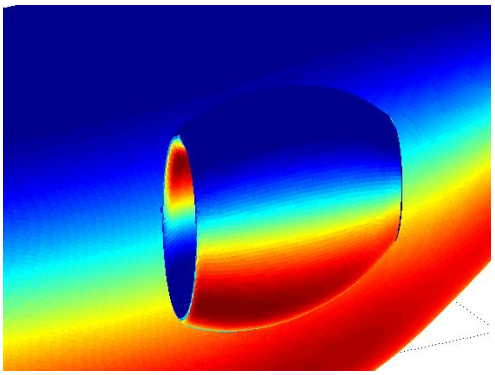

(b) Mesh of 1201860 elements

Fig. 22: Pressure distribution comparison

A numerical convergence study was also carried out on this geometry, to determine the accuracy of the solution produced by each mesh. This was done using the 3 meshes discussed earlier. By assuming the finest mesh to produce the correct solution, a comparison of each mesh with respect to this finest mesh was carried out to determine the errors in the solutions. By applying this to each of the meshes a convergence relationship can be calculated. The convergence plot with respect to the size of elements is shown in Figure 23.

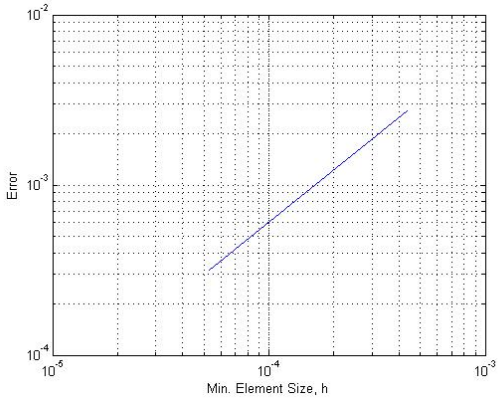

Fig. 23: convergence plot of Falcon

This produced a convergence rate (order) of 1.0287, with respect to the element size h and 0.8765, with respect to the number of elements N. These predicted orders of approximation of the model, however, are not entirely accurate. Due to the use of only 3 meshes in this convergence study, only 2 data points could be produced in order to get a comparison. This inherently creates a straight line on any plot and so any increasing rates of convergence (like in Figure 9 where the gradient of the line increases after the second point) between these two points are hidden. This could be further improved by carrying out the study with more meshes to produce a more accurate gradient and therefore order prediction.

4 Conclusion

The production of a MATLAB code has provided a useful tool for the rapid evaluation of aerodynamic geometries, particularly for the application of conceptual space craft design. It has also enabled the study of Newtonian flow theory and its applicability to hypersonic flow, and has concluded that:

Simple Newtonian flow theory becomes exact for hypersonic flow regimes where $M_\infty \to \infty$ and $\gamma \to 1$. This method analyses the aerodynamic performance with respect to surface pressure and so can determine the pressure and wave drag coefficients with suitable accuracy.

The Newtonian flow model results in a first (1.3146) order approximation with respect to both h and N. However, with the application of this selective refinement algorithm the order of approximation with respect to N is increased to a 1.4948 order. This suggests that while the same element size h is required, for both linear and selective refinement, the number of elements N can be limited due to the shadowing effect. The results for convergence rates with respect to both h and N for the 2D and 3D applications are summarised in table 1.

TABLE 1: Convergence order predictions with respect to the analytical solutions

Refinement scheme	Convergence order	
	$2D$	$3D$
h	1.3146	1.4207
N	1.4948	1.9410

The results show that the convergence rates for the 3D application are better than that of 2D. Therefore this suggests that the Newtonian model is quicker to converge for the 3D case where blunt bodies are used. This is because of the approximation of the pressure coefficient at the stagnation point as a result of a normal shock wave, created by blunt bodies at speeds above Mach 1.

The model is capable of handling complex geometries with fine meshes consisting of a vast number of elements, approximately 1.2 million. The runtime of this mesh was in the region of 30 minutes, using an Intel i3 core processor (2.2GHz), whereas the mesh consisting of 42720 took around 1 minute to run. This is still an acceptable runtime for the evaluation of a full 3D aircraft configuration to a high level of accuracy and shows that this model is a very useful tool in the concept design phase. Improvements in the runtime could be made by applying the selective refinement algorithm to the 3D case.

The limitations in the model, however, are the lack of continuum solution in the fluid surrounding the body and so is incapable of predicting the flow parameters and shock patterns. However, regardless of this lack of detail in the fluid continuum surrounding the body, this method produces a valid set of results for the aerodynamic performance. The Newtonian flow model is, therefore, a valid method for the use of a rapid evaluation tool during the design phase of hypersonic (re-entry) vehicles.

An interesting further point to note would be the comparison of the Newtonain model to other numerical models [9]. For further studies using high fidelity models see also [3] [4] [8].

ACKNOWLEDGEMENTS

I would like to thank Professor Ken Morgan for his guidance throughout the project. I would also like to thank Professor Oubay Hassan for his continued support in the project.

REFERENCES

[1] Dr. S. Sanz Fernández de Córdoba,"The 100 km Boundary for Astronautics", Fédération Aéronautique Internationale (FAI) Press Release, 2004, http://www.fai.org/icare-records/100km-altitude-boundary-for-astronautics

[2] John D. Anderson, Fundamentals of Aerodynamics, 1984

[3] Frédéric L. Chalot and Thomas J. R. Hughes, Analysis of hypersonic flows in thermochemical equilibrium by application of the Galerkin least-squares formulation, ICIAM, 1991

[4] Jose Fernando Padilla, Assessment of Gas-Surface Interaction Models for Computation of Rarefield Hypersonic Flows, 2008

[5] http://www.astronautica.ro/space/tag/re-entry-capsule/

[6] Dr. Jon Watmuff, AERO2463 Computation Engineering Analysis Matlab Assignment: Newtonian Theory, 2012

[7] Michael J. Grant and Robert D. Braun, Analytical Hypersonic Aerodynamics for Conceptual Design of Entry Vehicles, 2010

[8] H. Ahmadikia and E. Shirani, Numerical Simulation of Thermo-Chemical Non-Equilibrium Hypervelocity Flows, Journal of Applied Sciences 4(1): 110-117 ISSN 1607-8926, 2004

[9] Chester Ong, R.D. Braun and S.M.Ruffin, A survey of Hypersonic Aerodynamics and Aerothermodynamics for Planetary Re-Entry Capsules